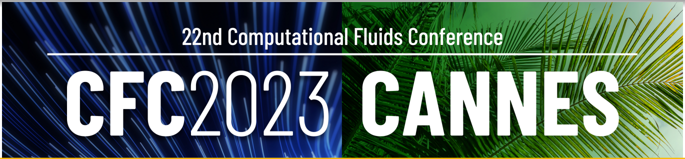

Towards efficient simulation of turbulent flows and noise in rotating machines

I. Abalakin[1], V. Bobkov[1], V. Tsvetkova[1], B. Sauvage[2], F. Miralles[3], T. Kozubskaya[1], S.F. Wornom[3], B. Koobus[3], A. Dervieux[2,4,*]

[1]CAALAB, Keldysh Institute of Applied Mathematics, Moscow, [2]Univ. Côte d'Azur/INRIA, Sophia-Antipolis, France, [3]IMAG, Univ. Montpellier, CNRS, Place Eugène Bataillon, 34090 Montpellier, [4]Lemma, Biot, France
This work was supported by the ANR NORMA project, grant ANR-19-CE40-0020-01 of the French National Research Agency.

Motivations

In the future, drones, manned drones and helicopters may have a more important role in cities, in particular if the noise produced is highly reduced. The noise of wind turbines is also a concern for the next years.
A bi-national cooperation started in 2019 addresses the numerical computation of the noise of rotors.
The French team studies new turbulence modeling (cf. the talk of Florian Miralles in this MS), and automatic anisotropic mesh adaptation: *Part A of this presentation*.
The Russian team studies numerical problems related to the turning geometries and massive calculations of turbulence and acoustics: *Part B of this presentation*.

A1: Anisotropic mesh adaptation (NiceFlow/Lemma)

- Vertex-centered FVM on tetrahedra.
- Multiple Reference Frame for rotation.
- Spalart-Allmaras RANS and DDES.
- An anisotropic *metric-based mesh adaptator*.

Metric $\mathscr{M}$:

$$\mathbf{x} \in \Omega \;\mapsto\; \mathscr{M}(\mathbf{x})$$

$\forall \mathbf{x}, \;\; \mathscr{M}(\mathbf{x})$ is a symmetric positive definite 3×3 matrix.

$$\mathscr{M} \;\mapsto\; \mathscr{H}, \text{ unit mesh}$$

- the rotation matrix diagonalizing it gives the stretching directions,
- the eigenvalues give the stretching strengths.
- the complexity $N = \mathscr{C}(\mathscr{M})$ is approximatively the number of vertices.

Error analysis of the RANS equations $\quad\Rightarrow\quad$ metric $\mathscr{M}$,
namely here: $|\pi M - M|, \quad M$, Mach number.

A1: Anisotropic mesh adaptation (for rotating frames)

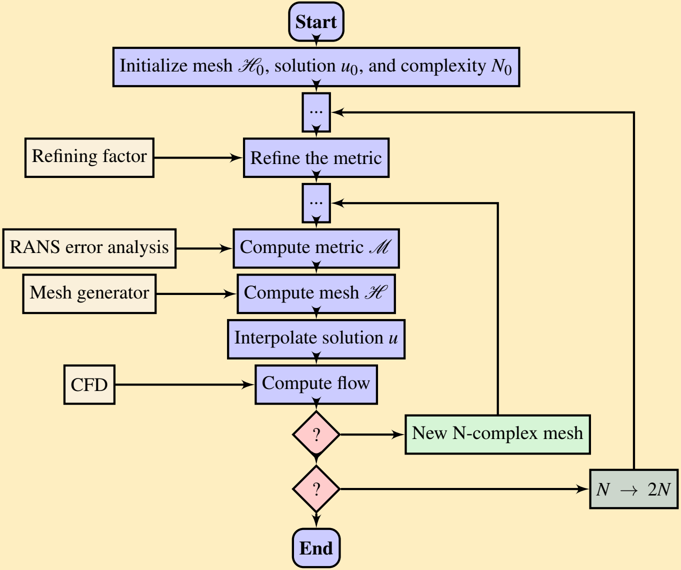

A2: Caradonna-Tung rotor (*)

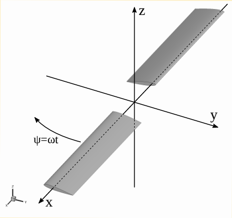

- Rotor radius is $R = 1.143m$.
- Blade section is a NACA0012 airfoil.
- The blade chord is $0.1905m$ and pitch angle is 8 degrees.
- The rotor rotation frequency is $650RPM$, tip velocity $77.8m/s$.
- The R-based Reynolds number is $Re = 5.9\ 10^6$.
- Mesh adaptation is based on the interpolation error for the Mach number.

(*) F. X. Caradonna and C. Tung. Experimental and analytical studies of a model helicopter rotor in hover. Technical Report NASA-TM-81232, NASA, Ames ResearchCenter, Moffett Field, California, September 1981.

A2: Caradonna-Tung rotor

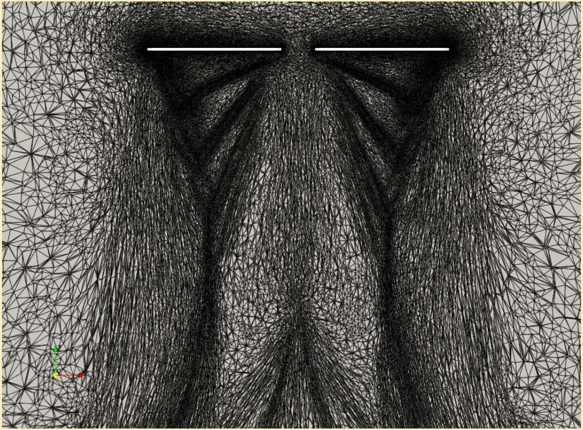

Anisotropic adapted mesh for the Caradonna-Tung rotor, 3M vertices.

A3: Caradonna-Tung rotor: velocity magnitude

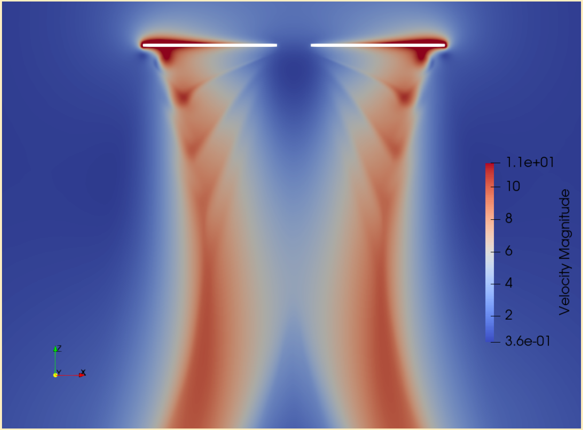

Velocity magnitude.

A4: Caradonna-Tung rotor: Q factor

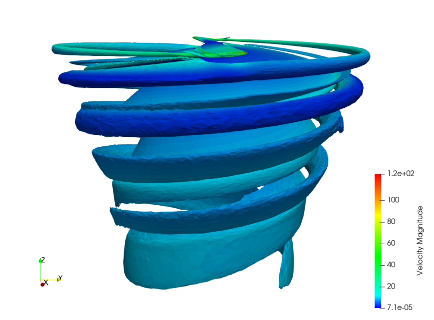

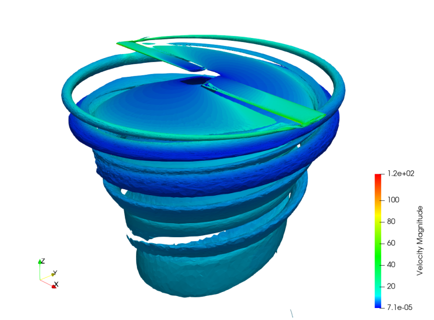

A4: Validation vs Caradonna-Tung measurements

$r/R = 0.5$

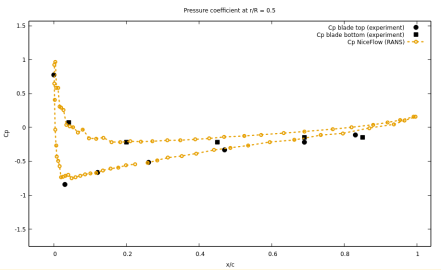

$r/R = 0.68$

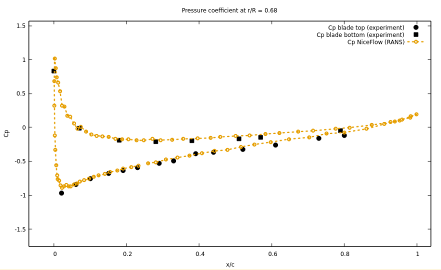

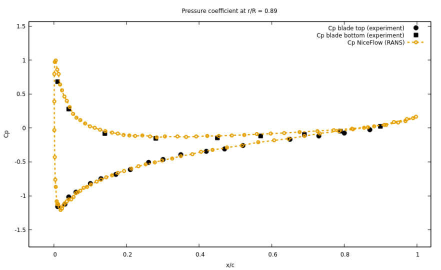

$r/R = 0.89$

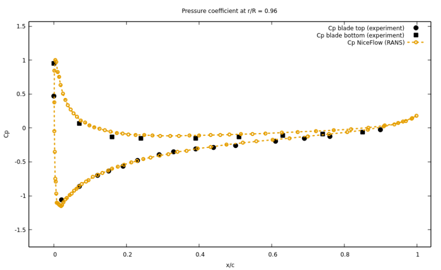

$r/R = 0.96$

A5: Caradonna-Tung/Robin combination

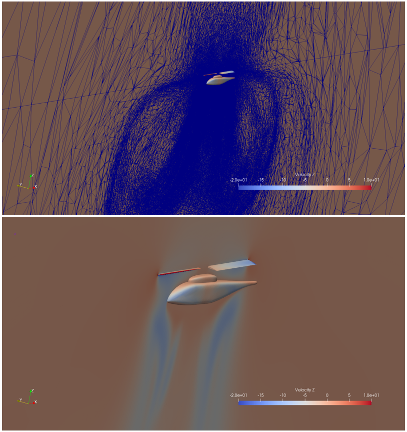

ROBIN fuselage with length 2R. The distance rotor plane/fuselage center of mass is $0.35m$. The fuselage pylon top/rotor plane gap is $0.125m$.

B1: Acoustic study, same geometry (code NOISEtte)

In order to capture at least the unsteady blade passing, a *sliding approach* and an *immersed boundary method* are compared.
Left, body-fitted mesh: 7.2M nodes (1.4M in rotor cylinder) 11K nodes on the fuselage surface.
Right, immersed boundary method mesh: 8.3M nodes (2.5M in rotor cylinder) 350K nodes on the fuselage surface.

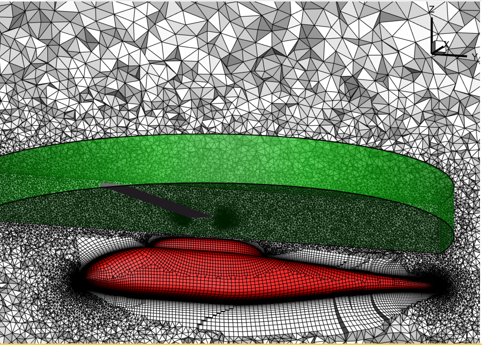

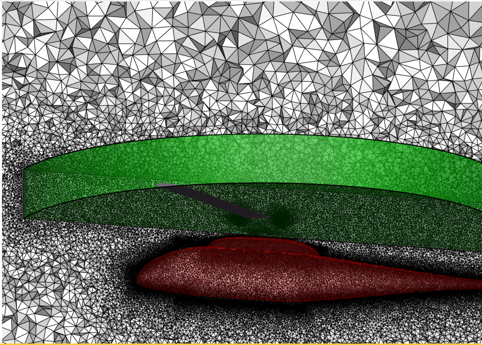

B2: Edge-Based reconstruction and sliding approximation

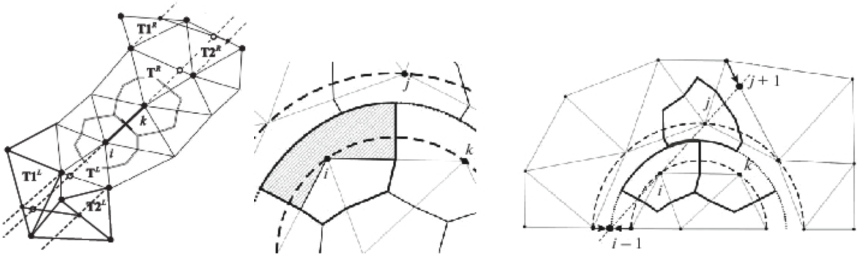

Left:

High-order Edge-Based Reconstruction is applied to improve the accuracy of interface values.

Center and right:

Sliding is organized inside an intermediate zone where interfaces are lying on the surface of a cylinder.

B3: Immersed Boundary Method of Brinkman

$$\Omega_{IBM} = \Omega_f(t) \cup \overline{\Omega}_B(t)$$

$$\mathbf{Q} = (\rho, \rho\mathbf{u}, E, \rho\tilde{\nu})^T$$

$$\frac{\partial \mathbf{Q}}{\partial t} + \nabla \cdot (\mathscr{F}^C(\mathbf{Q}) - \mathscr{F}^D(\mathbf{Q}, \nabla\mathbf{Q})) = \mathbf{S}(\mathbf{Q}, \nabla\mathbf{Q}).$$

$$\mathbf{S}^{penal}(\mathbf{Q}, \nabla\mathbf{Q}) = \mathbf{S}(\mathbf{Q}, \nabla\mathbf{Q}) + \left(0,\ \frac{\chi}{\eta}\rho(u_i - u_{Bi}),\ \frac{\chi}{\eta}\rho u_i(u_i - u_{Bi}),\ 0\right),$$

$$\chi(x,t) = \begin{cases} 1,\ x \in \overline{\Omega}_B(t) \\ 0,\ x \in \Omega_f(t). \end{cases}$$

In practice $\eta = 10^{-4}$.

B4: Validation (rotor alone)

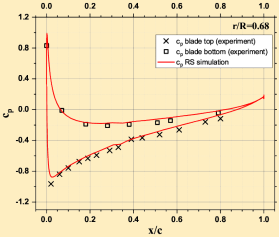

$r/R = 0.68$

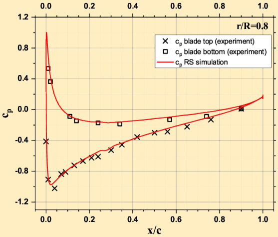

$r/R = 0.80$

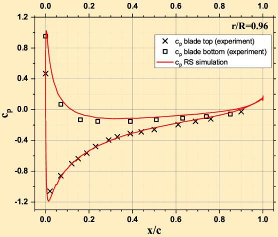

$r/R = 0.96$

Validation of Edge-Based-Reconstruction (rotor alone)

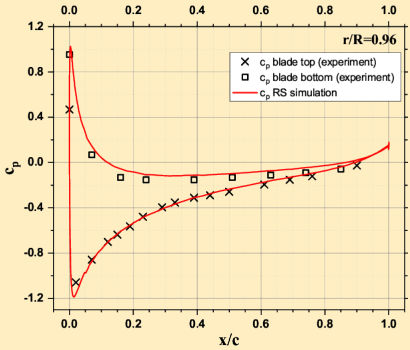

Validation of anisotropic adaptation (rotor alone)

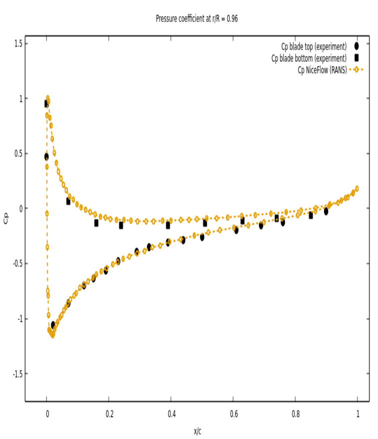

B5: analysis of combination, sliding

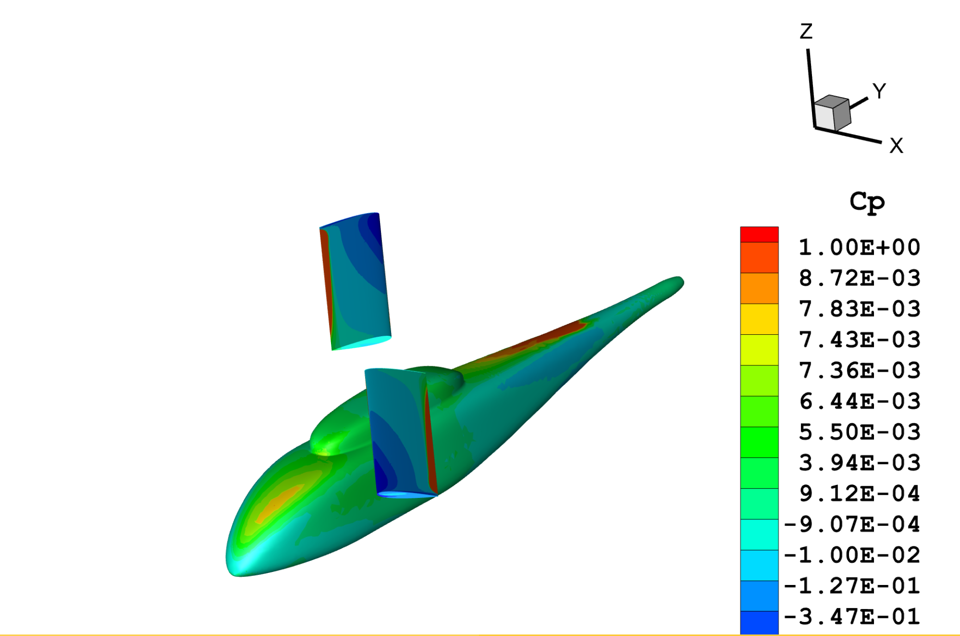

B5: analysis of combination, immersed boundary

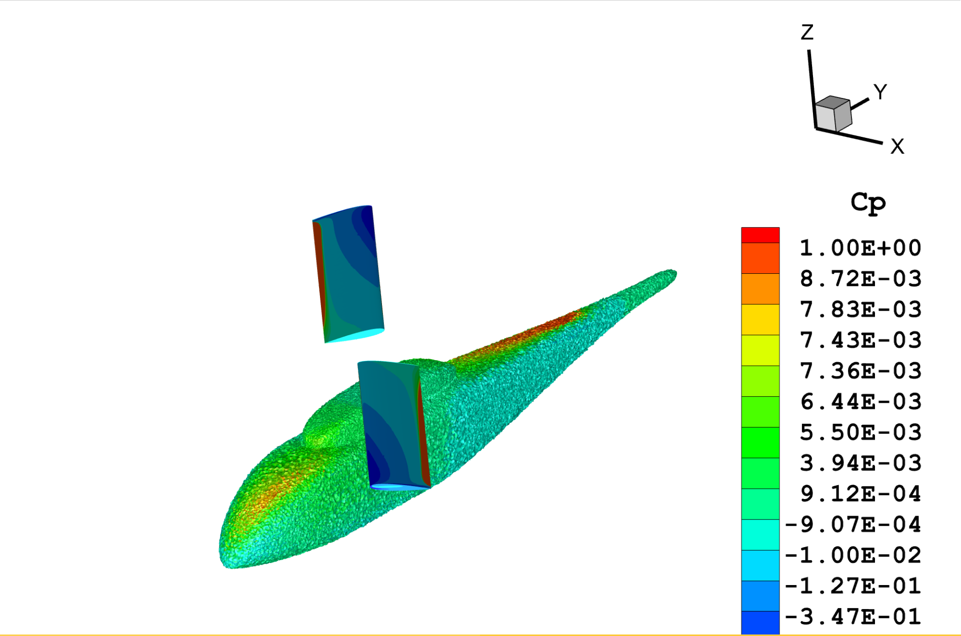

B6: Pressure analysis

BPF: blade passing frequency is 21.6 Hz.

PS: Pressure pulsations spectrum is $PS(\mathbf{x},f) = \frac{1}{2\pi} \int_{-\infty}^{+\infty} \frac{p(\mathbf{x},t)}{p_0} e^{-i2\pi f} dt$.

OASPL: overall sound pressure level is $OASPL = 10log_{10}\left[\int (PS(\mathbf{x},f))^2 dt\right]$.

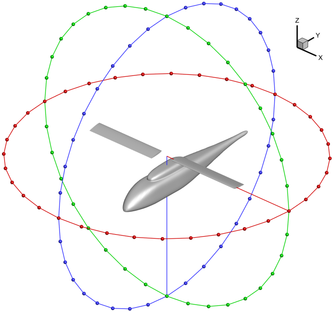

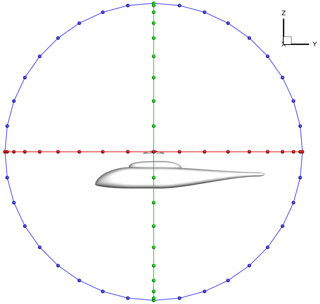

The sets of probes for acoustic field measurements: red: XY plane, green: XZ plane, blue: YZ plane (every 10 degrees).

B6ter: Pressure pulsation spectra (rotor alone)

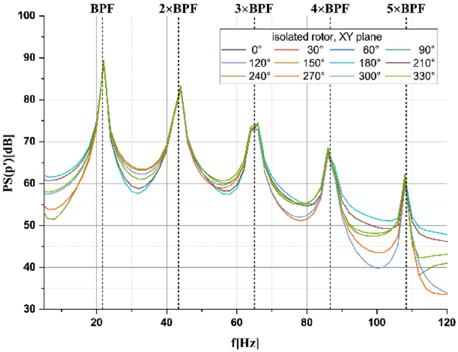

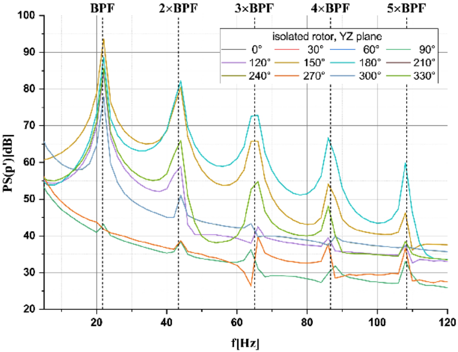

Right size XY plane, left YZ plane. Lowest curves are for 90 deg. and 270 deg.

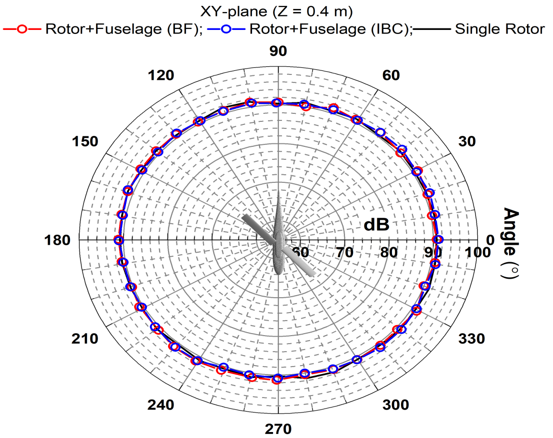

OASPL directivity diagram, XY.

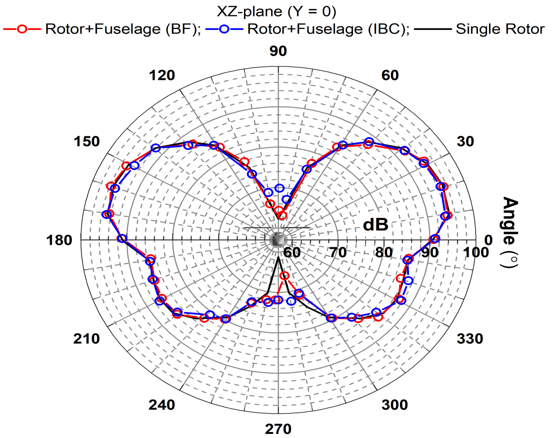

OASPL directivity diagram, XZ.

B9: analysis

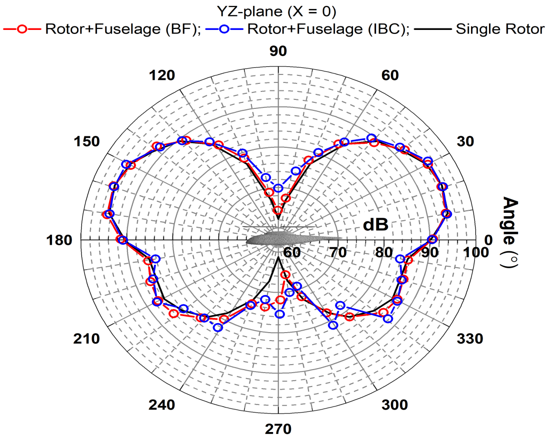

OASPL directivity diagram, YZ.

B10: Concluding remarks

The mesh-adaptative approach permits a global computation and easier shape optimization. We are developping two new extensions. In the first extension the hybrid turbulence model is completed by an intermittency equation in order to improve the prediction of transition, see the talk of F. Mirales in this session. In the second extension, the mesh adaptation is extended to space-time adaptation, see the talk of B. Sauvage in MS6-03A, in order to adapt space-time the LES computations.

The second part validates sliding and immersed boundary condition for an acoustic prediction. The fuselage influences slightly the directivity in the directions towards the ground.

Both teams are working towards the capturing of vortices after the blades and the noise created by them.